

## Evaluation of the Effect of Consciousness Energy Healing Treatment on the Physicochemical and Thermal Properties of Selenium

Gopal Nayak<sup>1</sup>, Mahendra Kumar Trivedi<sup>1</sup>, Alice Branton<sup>1</sup>, Dahryn Trivedi<sup>1</sup>, Snehasis Jana<sup>2,\*</sup>

<sup>1</sup> Trivedi Global, Inc., Henderson, USA.

<sup>2</sup> Trivedi Science Research Laboratory Pvt. Ltd., Bhopal, India.

### Abstract

Selenium is an essential micronutrient required for healthy metabolism, as well as prevention, and treatment of selenium deficiency diseases. The experiment aimed to evaluate the influence of the Trivedi Effect<sup>®</sup>-Consciousness Energy Healing Treatment on the physicochemical and thermal properties of selenium using modern analytical techniques. The selenium sample was divided into two parts, one part of the test sample was called the control sample, while the second part of the test sample received the Biofield Treatment remotely by a renowned Biofield Energy Healer, Gopal Nayak, and was called the treated sample. The particle size values were significantly decreased by 37.69% ( $d_{10}$ ), 14.36% ( $d_{50}$ ), 4.31% ( $d_{90}$ ), and 11.58% [D(4,3)], hence, the specific surface area was significantly increased by 33.64% in the treated sample compared to the control sample. The PXRD peak intensities and crystallite sizes were significantly altered ranging from 5.23% to 100% and 75% to 111.7%, respectively; whereas 7.81% significantly decreased the average crystallite size in the treated sample than the control sample. The latent heat of fusion of the treated sample was significantly increased by 12.37% compared with the control sample. The results suggested that the Trivedi Effect<sup>®</sup> might generate a new polymorphic form of selenium which would offer better solubility, bioavailability and be thermally more stable compared with the control sample. The Biofield Treated selenium would be more useful to design novel nutraceutical/pharmaceutical formulations and might offer an enhanced therapeutic response against cardiovascular disease, cancer, neuromuscular disorders, diabetes, stress, aging, male infertility, viral diseases, degenerative ailments, etc.

**Corresponding Author:** Snehasis Jana, Trivedi Science Research Laboratory Pvt. Ltd., Bhopal, India. Tel: +91-022-25811234; Email: [publication@trivedieffect.com](mailto:publication@trivedieffect.com)

**Running Title:** Impact of Consciousness Energy Treatment on Selenium

**Keywords:** Selenium, The Trivedi Effect<sup>®</sup>, Consciousness Energy Healing Treatment, Complementary and Alternative Medicine, Particle size, Surface area, PXRD, DSC

**Received:** Aug 22, 2018

**Accepted:** Sep 20, 2018

**Published:** Sep 24, 2018

**Editor:** Weihe Zhang, The University of North Carolina at Chapel Hill, USA.

## Introduction

Selenium (Se) is an essential trace element nutrient for humans and animals. It regulates a healthy metabolism and inhibits the toxic effects of heavy metals in the body [1]. The rich natural sources for Se are meat, fish, mushrooms, cereals, nuts, etc. This can be obtained from mineral supplements [1,2]. It is one of the key components of unusual amino acids selenocysteine and selenomethionine; selenium enzymes, and about 30 selenoproteins [3]. It is a potent antioxidant, which protects against oxidative damage, infections, nervous system; plays critical roles in reproduction, DNA synthesis, and thyroid hormone metabolism [1,4,5]. A poor selenium containing diet and/or genetic problems may lead to selenium deficiency in the body [6]. Se deficiency in the body is responsible for the critical pathophysiology of many diseases, i.e., cancer, diabetes, male infertility, muscle disorders, neurological disorders, cardiovascular disease, degenerative ailments, viral diseases, etc. [7-9]. Therefore, Se is recommended as a daily supplement in a number of countries. But, excess intake of Se may cause adverse health effects [9,10]. It is absorbed by the body in the form selenite which is more than 80 percent.

The physicochemical properties of any pharmaceutical/nutraceutical compound play a crucial role in its stability, solubility, bioavailability, and therapeutic efficacy in the body [11]. The biggest challenge for pharmaceutical scientists is improving the quality of pharmaceutical/nutraceutical compounds for better therapeutic efficacy. Scientifically, the Trivedi Effect<sup>®</sup>-Consciousness Energy Healing Treatment (Biofield Energy Healing Treatment) has been proven to have a significant impact on the particle size, surface area, thermal properties, and bioavailability of pharmaceutical and nutraceutical compounds [12-14]. The Trivedi Effect<sup>®</sup> is a natural and the only scientifically proven phenomenon in which an expert can harness this inherently intelligent energy from the Universe and transmit it anywhere on the planet through the possible mediation of neutrinos [15]. "Biofield" is a unique, infinite, para-dimensional electromagnetic field exists surrounding the body, originating from the continuous movements of the charged particles, ions, cells, blood/lymph flow, brain functions, heart function, etc. This

Biofield Energy Therapy (energy medicine) has been reported to have substantial outcomes against various disease conditions and to maintain the overall quality of life [15,16]. The National Institutes of Health/National Center for Complementary and Alternative Medicine (NIH/NCCAM) recommend and included the Energy therapy under the Complementary and Alternative Medicine (CAM) category along with other therapies, medicines and practices such as Ayurvedic medicine, naturopathy, homeopathy, Qi Gong, Tai Chi, yoga, chiropractic/osteopathic manipulation, meditation, massage, acupuncture, acupressure, hypnotherapy, Reiki, Roling structural integration, mindfulness, aromatherapy, cranial sacral therapy, applied prayer, etc. The CAM has been accepted by the most of the U.S. population with several advantages [17,18]. Similarly, the Trivedi Effect<sup>®</sup> Treatment also has a significant impact on the characteristic properties of the metals, ceramics, and polymers, organic compounds, crops, livestock, microorganisms, and cancer cells [19-29]. These outstanding experimental results motivated the authors to determine the impact of the Trivedi Effect<sup>®</sup>-Consciousness Energy Healing Treatment on the physicochemical and thermal properties of selenium using particle size analysis (PSA), powder X-ray diffraction (PXRD), and differential scanning calorimetry (DSC).

## Materials and Methods

### Chemicals and Reagents

The selenium (Se) powder sample was procured from Sigma Aldrich, USA and the other chemicals required during the experiments were of the analytical standard available in India.

### Consciousness Energy Healing Treatment Strategies

The test sample Se powder used in the experiment was divided into two parts. One part of the Se powder sample was received the Trivedi Effect<sup>®</sup>-Consciousness Energy Healing Treatment remotely under standard laboratory conditions for 3 minutes by the renowned Biofield Energy Healer, Gopal Nayak, India, known as the treated sample. The second part of the sample did not receive the Biofield Energy Treatment and was called the control sample. Further, the control sample was treated with "sham" healer for

the comparison purposes. The “sham” healer did not have any knowledge about the Biofield Energy Treatment. The Biofield Energy Treated sample and untreated Se powder sample were both kept in sealed conditions and characterized using PSA, PXRD, and DSC analytical techniques.

### Characterization

#### Particle Size Analysis (PSA)

The particle size analysis of Se powder was performed with the help of Malvern Mastersizer 2000, of the UK, with a detection range between 0.01 μm to 3000 μm using the wet method [30, 31]. The sample unit (Hydro MV) was filled with a sunflower oil dispersant medium and the stirrer operated at 2500 rpm. Particle size distribution analysis of Se powder was performed to obtain the average particle size. Where,  $d$  (0.1) μm,  $d(0.5)$  μm,  $d(0.9)$  μm represent particle diameter corresponding to 10%, 50%, and 90% of the cumulative distribution.  $D(4,3)$  represents the average mass-volume diameter, and SSA is the specific surface area (m<sup>2</sup>/g). The calculations were done by using software Mastersizer Ver. 5.54.

The percent change in particle size ( $d$ ) for Se powder at below 10% level ( $d_{10}$ ), 50% level ( $d_{50}$ ), 90% level ( $d_{90}$ ), and  $D(4,3)$  was calculated using the following equation 1:

$$\% \text{ change in the particle size} = \frac{[d_{\text{Treated}} - d_{\text{Control}}]}{d_{\text{Control}}} \times 100 \quad (1)$$

Where  $d_{\text{Control}}$  and  $d_{\text{Treated}}$  are the particle sizes (μm) at below 10% level ( $d_{10}$ ), 50% level ( $d_{50}$ ), and 90% level ( $d_{90}$ ) of the control and the Biofield Energy Treated samples, respectively.

The percent change in surface area ( $S$ ) was calculated using the following equation 2:

$$\% \text{ change in the surface area} = \frac{[S_{\text{Treated}} - S_{\text{Control}}]}{S_{\text{Control}}} \times 100 \quad (2)$$

Where  $S_{\text{Control}}$  and  $S_{\text{Treated}}$  are the surface area of the control and the Biofield Energy Treated Se, respectively.

#### Powder X-ray Diffraction (PXRD) Analysis

The PXRD analysis of Se powder sample was executed with the help of Rigaku MiniFlex-II Desktop X-ray diffractometer (Japan) [32, 33]. The Cu K $\alpha$  radiation source tube output voltage and output current were 30 kV and 15 mA, respectively. Scans were

performed at room temperature. The size of individual crystallites was calculated from PXRD data using the Scherrer's formula (3)

$$G = k\lambda/\beta\cos\theta \quad (3)$$

Where  $k$  is the equipment constant (0.94),  $G$  is the crystallite size in nm,  $\lambda$  is the radiation wavelength (0.154056 nm for K $\alpha$ 1 emission),  $\beta$  is the full-width at half maximum (FWHM), and  $\theta$  is the Bragg angle [34].

The percent change in crystallite size ( $G$ ) of Se was calculated using the following equation 4:

$$\% \text{ change in the crystallite size} = \frac{[G_{\text{Treated}} - G_{\text{Control}}]}{G_{\text{Control}}} \times 100 \quad (4)$$

Where  $G_{\text{Control}}$  and  $G_{\text{Treated}}$  are the crystallite size of the control and the Biofield Energy Treated samples, respectively.

#### Differential Scanning Calorimetry (DSC)

The DSC analysis of Se powder sample was performed with the help of DSC Q200, TA instruments. Sample of ~1-2 mg was loaded to the aluminium sample pan at a heating rate of 10°C/min from 30°C to 350°C [30, 31]. The % change in melting point ( $T$ ) was calculated using the following equation 5:

$$\% \text{ change in the melting point} = \frac{[T_{\text{Treated}} - T_{\text{Control}}]}{T_{\text{Control}}} \times 100 \quad (5)$$

Where  $T_{\text{Control}}$  and  $T_{\text{Treated}}$  are the melting point of the control and the Biofield Energy Treated samples, respectively.

The percent change in the latent heat of fusion ( $\Delta H$ ) was calculated using following equation 6:

$$\% \text{ change in the latent heat of fusion} = \frac{[\Delta H_{\text{Treated}} - \Delta H_{\text{Control}}]}{\Delta H_{\text{Control}}} \times 100 \quad (6)$$

Where  $\Delta H_{\text{Control}}$  and  $\Delta H_{\text{Treated}}$  are the latent heat of fusion of the control and the Biofield Energy Treated Se, respectively.

## Results and Discussion

#### Particle Size Analysis (PSA)

The particle size distribution analysis data of both the control and the Biofield Energy Treated Se powder samples are presented in Table 1. The particle size values of the control Se powder at  $d_{10}$ ,  $d_{50}$ ,  $d_{90}$ , and  $D(4,3)$  were 9.859 μm, 26.595 μm, 53.601 μm, and

Table 1. Particle size distribution of the control and Biofield Energy Treated selenium.

Parameter	d <sub>10</sub> (µm)	d <sub>50</sub> (µm)	d <sub>90</sub> (µm)	D(4,3) (µm)	SSA (m <sup>2</sup> /g)
Control	9.859	26.595	53.601	29.513	0.324
Biofield Treated	6.143	22.775	51.29	26.095	0.433
Percent change* (%)	-37.69	-14.36	-4.31	-11.58	33.64

d<sub>10</sub>, d<sub>50</sub>, and d<sub>90</sub>: particle diameter corresponding to 10%, 50%, and 90% of the cumulative distribution, D(4,3): the average mass-volume diameter, and SSA: the specific surface area. \*denotes the percentage change in the Particle size distribution of the Biofield Energy Treated sample with respect to the control sample.

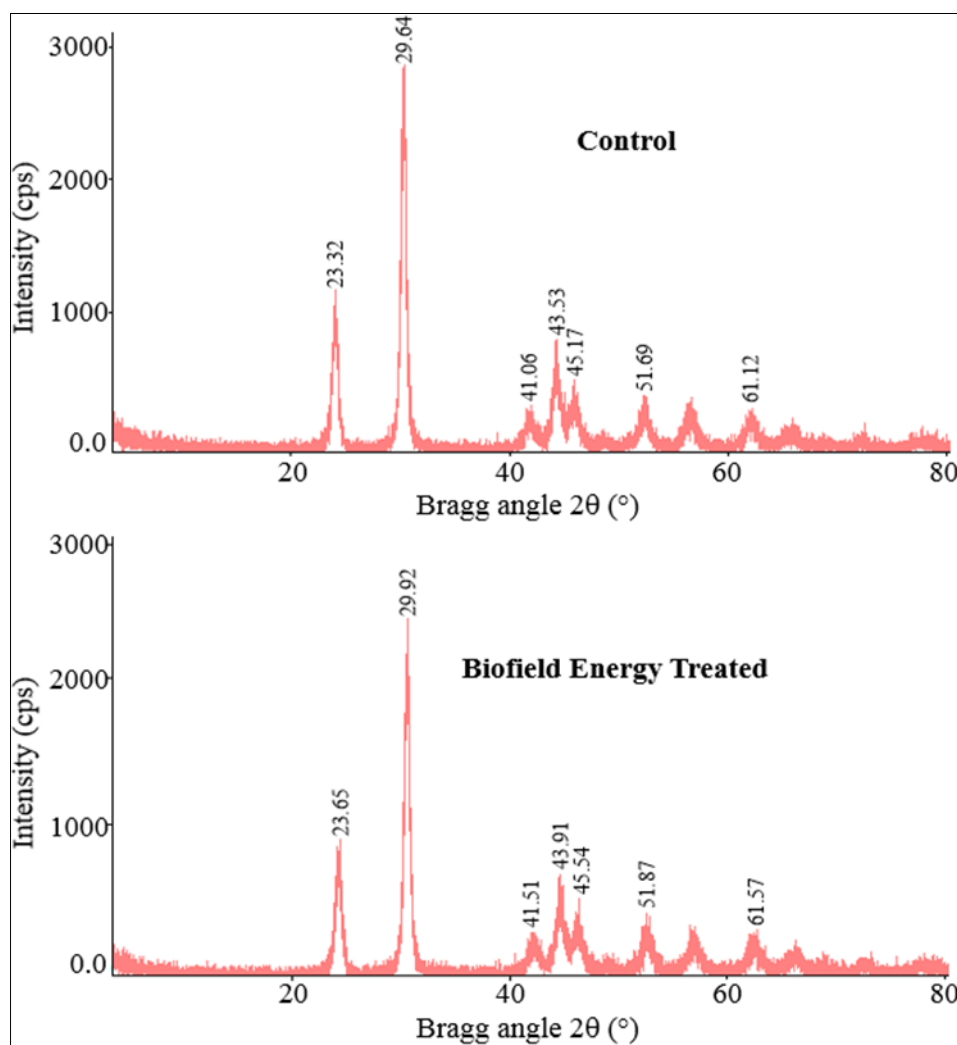


Figure 1. XRD diffractograms of the control and Biofield Energy Treated selenium powder.

29.513  $\mu\text{m}$ , respectively. Similarly, the particle sizes of the Biofield Energy Treated sample at  $d_{10}$ ,  $d_{50}$ ,  $d_{90}$ , and  $D(4,3)$  were 6.143  $\mu\text{m}$ , 22.775  $\mu\text{m}$ , 51.29  $\mu\text{m}$ , and 26.095  $\mu\text{m}$ , respectively. The particle size values of the Biofield Energy Treated Se sample were significantly decreased by 37.69%, 14.36%, 4.31%, and 11.58% at  $d_{10}$ ,  $d_{50}$ ,  $d_{90}$ , and  $D(4,3)$ , respectively compared to the control sample. Therefore, the specific surface area of the Biofield Energy Treated sample (0.433  $\text{m}^2/\text{g}$ ) was significantly increased by 33.64% compared with the control sample (0.324  $\text{m}^2/\text{g}$ ). The results suggested that the Trivedi Effect<sup>®</sup>-Consciousness Energy Healing Treatment might act as an external force for breaking larger particles to smaller one hence increasing the surface area of Se particles significantly. Pharmaceutical compounds with smaller particle size increase the surface area and improve the dissolution rate, and bioavailability in the body [11, 35]. Therefore, the Biofield Energy Treated Se powder would offer better solubility, bioavailability, and therapeutic efficacy compared to the untreated sample.

#### *Powder X-ray Diffraction (PXRD) Analysis*

The diffractogram of the control Se powder sample showed sharp and intense peaks at Bragg's angle ( $2\theta$ ) near to 23.32°, 29.64°, 41.06°, 43.53°, 45.17°, 51.69°, and 61.12° (Figure 1). Similarly, the diffractogram of the Biofield Energy Treated sample showed sharp and intense peaks at Bragg's angle ( $2\theta$ ) near to 23.65°, 29.92°, 41.51°, 43.91°, 45.54°, 51.87°, and 61.57° (Figure 1). The sharp and intense peaks of both the diffractograms specified that the samples were crystalline. The highest peak intensity of the control and Biofield Energy Treated sample were observed at  $2\theta$  equal to 29.64° and 29.92°, respectively (Table 2, entry 2). The peak intensities of the Biofield Energy Treated sample were significantly decreased in the range from 5.23% to 100% compared to the control sample. However, the crystallite sizes of the Biofield Energy Treated Se sample were significantly increased in the range from 75% to 111.7% compared to the control sample. Overall, the average crystallite size of the Biofield Energy Treated Se powder (96.94 nm) was significantly decreased by 7.81% compared to the control sample (105.16 nm).

As per the literature, the peak intensity of each

diffraction face on the crystalline compound changes according to the crystal morphology and alterations in the XRD pattern provide the proof of polymorphic transitions [36-38]. The Trivedi Effect<sup>®</sup>-Consciousness Energy Healing Treatment probably produced the new polymorphic form of Se through the mediation of neutrinos [15]. Different polymorphic forms of pharmaceuticals have significant effects on drug performance, such as bioavailability, therapeutic efficacy, and toxicity, because of their physicochemical properties are different from the original form [39, 40]. Therefore, the Trivedi Effect<sup>®</sup>-Consciousness Energy Healing Treated Se would be better in designing novel pharmaceutical and nutraceutical formulations.

#### *Differential Scanning Calorimetry (DSC) Analysis*

The thermal analysis has been performed to characterize the thermal behavior of the Biofield Energy Treated Se compared to the control sample (Table 3). The thermograms of both the control and Biofield Energy Treated sample showed sharp endothermic peaks at 222.1°C and 221.5°C, respectively (Figure 2). The melting point of the Biofield Energy Treated sample was slightly decreased by 0.27% compared with the control sample (Table 3).

The latent heat of fusion ( $\Delta H_{\text{fusion}}$ ) of the Biofield Energy Treated sample (78.23 J/g) was significantly increased by 12.37% compared with the control sample (69.62 J/g) (Table 3). The significant change in the  $\Delta H_{\text{fusion}}$  can be attributed to the change in the molecular chains and the crystal structure of that compound [41]. Thus, it can be assumed that the Biofield Energy Treatment might be responsible for the improved thermal stability of the treated Se sample compared to the control sample.

#### **Conclusion**

The Trivedi Effect<sup>®</sup>-Consciousness Energy Healing Treatment (Biofield Energy Treatment) showed significant effects on the crystallite size, particle size, surface area, and thermal properties of the selenium powder. The particle size values of the Biofield Energy Treated sample powder were significantly decreased by 37.69%, 14.36%, 4.31%, and 11.58% at  $d_{10}$ ,  $d_{50}$ ,  $d_{90}$ , and  $D(4,3)$ , respectively. Therefore, the specific surface area of the Biofield Energy Treatment sample was significantly increased by 33.64% compared to the

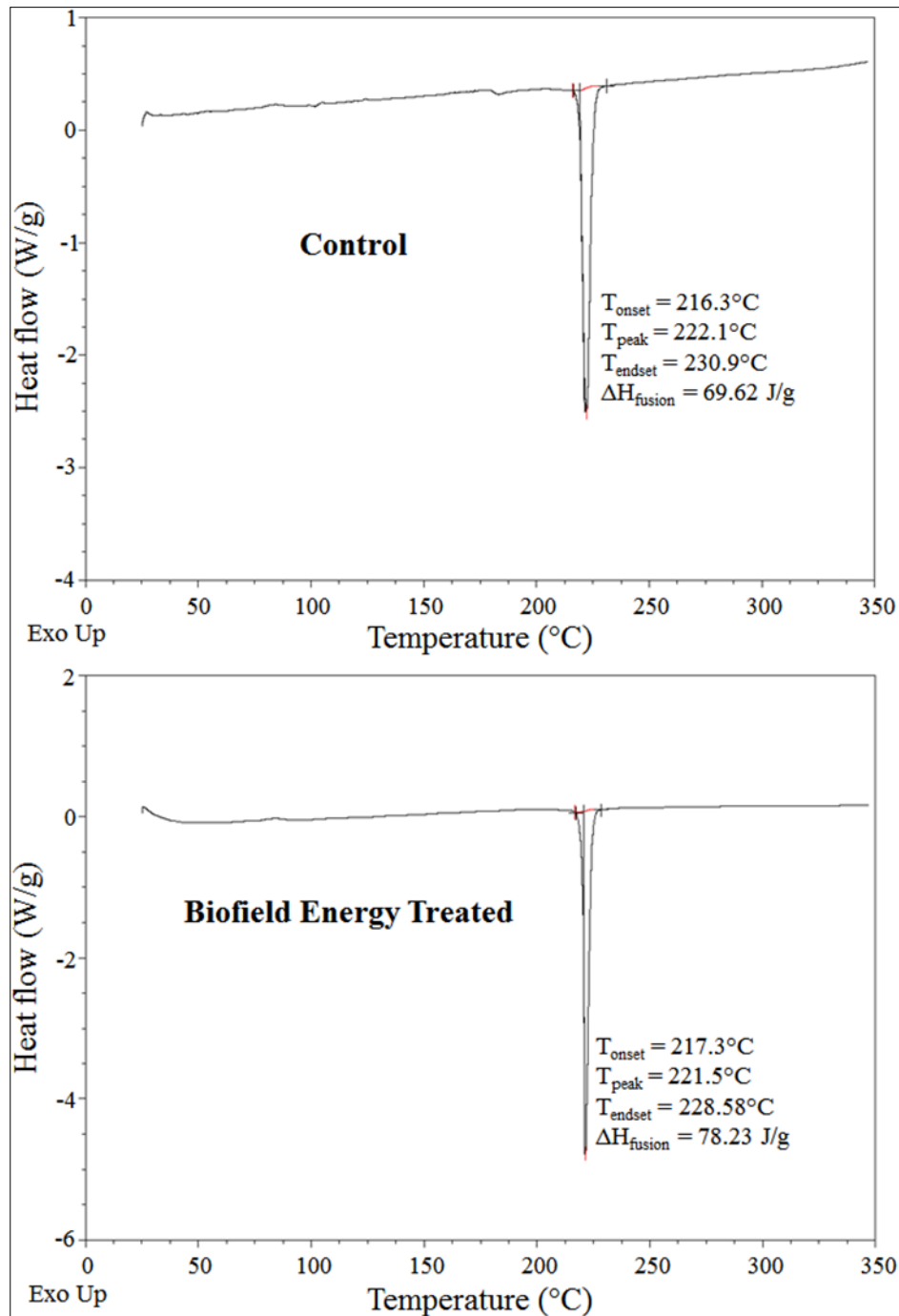


Figure 2. DSC thermograms of the control and Biofield Energy Treated selenium sample.



Table 2. PXRD data for the control and Biofield Energy Treated selenium powder.

Entry No.	Bragg angle ( $^{\circ}2\theta$ )		Peak Intensity (%)			Crystallite size (G, nm)		
	Control	Treated	Control	Treated	% change <sup>a</sup>	Control	Treated	% change <sup>b</sup>
1	23.32	23.65	514.00	401.00	-21.98	122.90	111.70	-9.11
2	29.64	29.92	1257.00	1056.00	-15.99	154.20	136.90	-11.22
3	41.06	41.51	153.00	145.00	-5.23	81.00	75.00	-7.41
4	43.53	43.91	347.00	313.00	-9.80	107.00	97.00	-9.35
5	45.17	45.54	243.00	214.00	-11.93	81.00	79.00	-2.47
6	51.69	51.87	206.00	140.00	-32.04	87.00	94.00	8.05
7	61.12	61.57	115.00	123.00	-100.00	103.00	85.00	-5.88
8	Average crystallite size					105.16	96.94	-7.81

<sup>a</sup>denotes the percentage change in the peak intensity of Biofield Energy Treated sample with respect to the control sample; <sup>b</sup>denotes the percentage change in the crystallite size of Biofield Energy Treated sample with respect to the control sample.

Table 3. DSC data for both control and Biofield Energy Treated samples of selenium sample.

Sample	Melting point ( $^{\circ}\text{C}$ )	$\Delta\text{H}$ (J/g)
Control Sample	222.1	69.62
Biofield Energy Treated	221.5	78.23
% Change*	-0.27	12.37

control sample. The PXRD peak intensities of the Biofield Energy Treatment sample were significantly decreased in the range from 5.23% to 100% compared with the control sample. However, the crystallite sizes of the Biofield Energy Treatment sample were significantly increased in the range from 75% to 111.7% compared to the control sample. But, the average crystallite size of the Biofield Energy Treatment sample was significantly decreased by 7.81% compared to the control sample. The melting point of the Biofield Energy Treatment sample was slightly altered, but the  $\Delta H_{\text{fusion}}$  significantly increased by 12.37% compared with the control sample. The results suggested that the Trivedi Effect<sup>®</sup>-Consciousness Energy Healing Treatment might generate a new polymorphic form of selenium which would offer better solubility, bioavailability and be thermally more stable compared with the control sample. The Biofield Energy Treated selenium would be more useful to design novel nutraceutical/ pharmaceutical formulations and which might offer enhanced therapeutic responses against cardiovascular disease, cancer, muscle disorders, neurological disorders, type-2 diabetes, viral diseases, stress, aging, male infertility, degenerative ailments, etc.

### Acknowledgements

The authors are grateful to Central Leather Research Institute, SIPRA Lab. Ltd., Trivedi Science, Trivedi Global, Inc., Trivedi Testimonials, and Trivedi Master Wellness for their assistance and support during this work.

### Conflict of Interest

Authors declare no conflict of interest.

### References

- Dietary Supplement Fact Sheet: Selenium. National Institutes of Health; Office of Dietary Supplements. Retrieved on 10-08-2018.
- Margaret, N.I.B., Allan, M.P., James, D. (1995) Selenium content of a range of UK food. *J. Food. Compos. Anal.* 8, 307-318.
- Stadtman, T.C. (1996) Selenocysteine. *Annu. Rev. Biochem.* 65, 83-100
- Li, X., Yin, D., Yin, J., Chen, Q., Wang, R. (2014) Dietary selenium protect against redox-mediated immune suppression induced by methylmercury exposure. *Food Chem. Toxicol.* 72, 169-177.
- Yang, X., Bao, Y., Fu, H., Li, L., Ren, T., et al. (2014) Selenium protects neonates against neurotoxicity from prenatal exposure to manganese. *PLoS one* 9, e86611.
- Brenneisen, P., Steinbrenner, H., Sies, H. (2005) Selenium, oxidative stress, health aspects. *Mol. Aspects Med.* 26, 256-267.
- Rayman, M.P. (2012) Selenium and human health. *The Lancet* 379, 1256-1268.
- Hatfield, D.L., Tsuji, P.A., Carlson, B.A., Gladyshev, V.N. (2014) Selenium and selenocysteine: Roles in cancer, health, and development. *Trends Biochem. Sci.* 39, 112-120.
- Romanm, M., Jitaru, P., Barbante, C. (2014) Selenium biochemistry and its role for human health. *Metallomics* 6, 25-54.
- Levander, O.A., Burk, R.F. (2006) Update of human dietary standards for selenium. In: Hatfield, D.L., Berry, M.J., Gladyshev, V.N., (Eds) *Selenium - Its molecular biology and role in human health*, Springer, New York.
- Chereson, R. (2009) Bioavailability, bioequivalence, and drug selection. In: Makoid C.M., Vuchetich, P.J., Banakar, U.V. (Eds) *Basic pharmacokinetics (1<sup>st</sup> Edn)* Pharmaceutical Press, London.
- Trivedi, M.K., Patil, S., Shettigar, H., Bairwa, K., Jana, S. (2015) Effect of biofield treatment on spectral properties of paracetamol and piroxicam. *Chem. Sci. J.* 6, 98.
- Trivedi, M.K., Branton, A., Trivedi, D., Nayak, G., Nykvist, C.D., et al. (2017) Evaluation of the Trivedi Effect<sup>®</sup>- Energy of Consciousness Energy Healing Treatment on the physical, spectral, and thermal properties of zinc chloride. *American Journal of Life Sciences.* 5: 11-20.
- Branton, A., Jana, S. (2017) Effect of The biofield energy healing treatment on the pharmacokinetics of 25-hydroxyvitamin D<sub>3</sub> [25(OH)D<sub>3</sub>] in rats after a single oral dose of vitamin D<sub>3</sub>. *American Journal of Pharmacology and Phytotherapy* 2, 11-18.
- Trivedi, M.K., Mohan, T.R.R. (2016) Biofield energy signals, energy transmission and neutrinos. *American Journal of Modern Physics* 5, 172-176.



16. Rubik, B., Muehsam, D., Hammerschlag, R., Jain, S. (2015) Biofield science and healing: history, terminology, and concepts. *Glob. Adv. Health Med.* 4, 8-14.
17. Barnes, P.M., Bloom, B., Nahin, R.L. (2008) Complementary and alternative medicine use among adults and children: United States, 2007. *Natl Health Stat Report* 12, 1-23.
18. Koithan, M. (2009) Introducing complementary and alternative therapies. *J. Nurse. Pract.* 5, 18-20.
19. Trivedi, M.K., Nayak, G., Patil, S., Tallapragada, R.M., Latiyal, O., et al. (2015) Impact of biofield treatment on atomic and structural characteristics of barium titanate powder. *Ind. Eng. Manage.* 4, 166.
20. Trivedi, M.K., Nayak, G., Patil, S., Tallapragada, R.M., Latiyal, O. (2015) Studies of the atomic and crystalline characteristics of ceramic oxide nano powders after bio field treatment. *Ind. Eng. Manage.* 4, 161.
21. Trivedi, M.K., Branton, A., Trivedi, D., Nayak, G., Mishra, R.K., et al. (2015) Characterization of physicochemical and thermal properties of biofield treated ethyl cellulose and methyl cellulose. *International Journal of Biomedical Materials Research* 3, 83-91.
22. Trivedi, M.K., Branton, A., Trivedi, D., Nayak, G., Sethi, K.K., et al. (2016) Isotopic abundance ratio analysis of biofield energy treated indole using gas chromatography-mass spectrometry. *Science Journal of Chemistry* 4, 41-48.
23. Trivedi, M.K., Branton, A., Trivedi, D., Nayak, G., Panda, P., et al. (2016) Evaluation of the isotopic abundance ratio in biofield energy treated resorcinol using gas chromatography-mass spectrometry technique. *Pharm. Anal. Acta.* 7, 481.
24. Sances, F., Flora, E., Patil, S., Spence, A., Shinde, V. (2013) Impact of biofield treatment on ginseng and organic blueberry yield. *AGRIVITA, Journal of Agricultural Science* 35, 22-29.
25. Trivedi, M.K., Branton, A., Trivedi, D., Nayak, G., Gangwar, M., et al. (2015) Agronomic characteristics, growth analysis, and yield response of biofield treated mustard, cowpea, horse gram, and groundnuts. *International Journal of Genetics and Genomics* 3, 74-80.
26. Trivedi, M.K., Branton, A., Trivedi, D., Nayak, G., Mondal, S.C., et al. (2015) Effect of biofield treated energized water on the growth and health status in chicken (*Gallus gallus domesticus*). *Poult. Fish Wildl. Sci.* 3, 140.
27. Trivedi, M.K., Branton, A., Trivedi, D., Shettigar, H., Nayak, G., et al. (2015) Antibiofilm, biochemical reactions and genotyping characterization of biofield treated *Staphylococcus aureus*. *American Journal of BioScience* 3, 212-220.
28. Trivedi, M.K., Branton, A., Trivedi, D., Nayak, G., Mondal, S.C., et al. (2015) Antimicrobial sensitivity, biochemical characteristics and biotyping of *Staphylococcus saprophyticus*: An impact of biofield energy treatment. *J. Women's Health Care* 4, 271.
29. Trivedi, M.K., Patil, S., Shettigar, H., Mondal, S.C., Jana, S. (2015) The potential impact of biofield treatment on human brain tumor cells: A time-lapse video microscopy. *J. Integr. Oncol.* 4, 141.
30. Trivedi, M.K., Sethi, K.K., Panda, P., Jana, S. (2017) A comprehensive physicochemical, thermal, and spectroscopic characterization of zinc (II) chloride using X-ray diffraction, particle size distribution, differential scanning calorimetry, thermogravimetric analysis/differential thermogravimetric analysis, ultraviolet-visible, and Fourier transform-infrared spectroscopy. *International Journal of Pharmaceutical Investigation* 7, 33-40.
31. Trivedi, M.K., Sethi, K.K., Panda, P., Jana, S. (2017) Physicochemical, thermal and spectroscopic characterization of sodium selenate using XRD, PSD, DSC, TGA/DTG, UV-vis, and FT-IR. *Marmara Pharmaceutical Journal* 21/2, 311-318.
32. Desktop X-ray Diffractometer "MiniFlex+" (1997) *The Rigaku Journal* 14: 29-36.
33. Zhang, T., Paluch, K., Scalabrino, G., Frankish, N., Healy, A.M., et al. (2015) Molecular structure studies of (1S,2S)-2-benzyl-2,3-dihydro-2-(1Hinden-2-yl)-1H-inden-1-ol. *J. Mol. Struct.* 1083, 286-299.
34. Langford, J.I., Wilson, A.J.C. (1978) Scherrer after sixty years: A survey and some new results in the determination of crystallite size. *J. Appl. Cryst.* 11, 102-113.

35. Zhao, Z., Xie, M., Li, Y., Chen, A., Li, G., et al. (2015) Formation of curcumin nanoparticles *via* solution-enhanced dispersion by supercritical CO<sub>2</sub>. Int. J. Nanomedicine 10, 3171-3181.
36. Inoue, M., Hirasawa, I. (2013) The relationship between crystal morphology and XRD peak intensity on CaSO<sub>4</sub>.2H<sub>2</sub>O. J Crystal Growth 380: 169-175.
37. Raza, K., Kumar, P., Ratan, S., Malik, R., Arora, S. (2014) Polymorphism: The phenomenon affecting the performance of drugs. SOJ Pharm. Pharm. Sci. 1, 10.
38. Brittain, H.G. (2009) Polymorphism in pharmaceutical solids in Drugs and Pharmaceutical Sciences, volume 192, 2<sup>nd</sup> Edn, Informa Healthcare USA, Inc., New York.
39. Censi, R., Martino, P.D. (2015) Polymorph Impact on the bioavailability and stability of poorly soluble drugs. Molecules 20, 18759-18776.
40. Blagden, N., de Matas, M., Gavan, P.T., York, P. (2007) Crystal engineering of active pharmaceutical ingredients to improve solubility and dissolution rates. Adv. Drug Deliv. Rev. 59, 617-630.
41. Zhao, Z., Xie, M., Li, Y., Chen, A., Li, G., et al. (2015) Formation of curcumin nanoparticles *via* solution-enhanced dispersion by supercritical CO<sub>2</sub>. Int. J. Nanomedicine 10: 3171-3181.